

2-MeBr and **2-MeI** is consistent with the observation of the exceptionally long Au-Br bond of **2-MeBr**. Halogen exchange may also involve a mixed valence Au(I)/Au(III) complex⁴² or oligomeric pairs of complexes. Further studies specifically addressing these possibilities are being pursued.

Acknowledgment. These studies are supported by the National Science Foundation, Grant CHE-8408414, the donors of the Petroleum Research Fund, as administered by the American

(42) Fackler, J. P., Jr.; Trzcinska-Bancroft, B. *Organometallics* 1985, 4, 1633-1637.

Chemical Society, and The Welch Foundation.

Registry No. 1, 50449-81-5; 1-MeI, 55927-69-0; 1-Br₂, 55873-02-4; 1-I₂, 55744-31-5; 1-SiI, 98678-29-6; 1-BzBr, 98678-30-9; 2, 81457-56-9; 2-MeI, 81457-57-0; 2-MeBr, 89462-48-6; 2-I₂, 81457-58-1; 2-SiI, 98678-28-5; 2-BzBr, 98687-67-3; 2-Br₂, 89462-50-0; 2-CD₃I, 89462-49-7; 2-Cl₂, 97571-09-0; MeI, 74-88-4; MeBr, 74-83-9; Me₃SiCH₂I, 4206-67-1; PhCH₂Br, 100-39-0; Br₂, 7726-95-6; I₂, 7553-56-2; CCl₄, 56-23-5; CD₃Br, 1111-88-2; CD₃I, 865-50-9; MeCl, 74-87-3; CD₃Cl, 1111-89-3.

Supplementary Material Available: Tables of thermal parameters, calculated hydrogen atom coordinates, bond lengths and bond angles, and structure factors (62 pages). Ordering information is given on any current masthead page.

Metal-Spine Conductivity in a Partially Oxidized Metallomacrocycle: (Phthalocyaninato)cobalt Iodide

Jens Martinsen,[†] Judith L. Stanton,[†] Richard L. Greene,[‡] Jiro Tanaka,[§] Brian M. Hoffman,^{*†} and James A. Ibers^{*†}

Contribution from the Department of Chemistry and Materials Research Center, Northwestern University, Evanston, Illinois 60201, IBM Research Laboratory, San Jose, California 95193, and the Department of Chemistry, Nagoya University, Chikusa, Nagoya, 464 Japan.
Received February 5, 1985

Abstract: Oxidation by iodine of (phthalocyaninato)cobalt(II), Co(pc), affords the title compound, Co(pc)I, which is comprised of metal-over-metal columnar stacks of partially (¹/₃) oxidized Co(pc) groups that are surrounded by chains of I₃⁻ ions. Co(pc)I crystallizes in space group *D*_{2h}²-*P4/mcc* of the tetragonal system with *a* = 13.927 (1) Å, *c* = 6.247 (1) Å, *V* = 1212 Å³, and *Z* = 2. The value of *R* on *F*_o² for 66 variables and 540 observations is 0.055. Results of physical measurements, in particular the sign of the thermoelectric power, show the metal centers to be the site of oxidation. Charge transport thus proceeds along one-dimensional chains of metal atoms, as in the linear-chain platinum compounds. Strong interactions among the partially oxidized metal centers of the cobalt spine force the Co(pc) subunits to adopt an anomalously small interplanar spacing (3.12 Å). They lead to an approximately temperature-independent susceptibility that is associated with strong Coulomb correlations in a one-dimensional cobalt d_{z²} band. The room-temperature conductivity of Co(pc)I is $\sigma \sim 50 \Omega^{-1} \text{cm}^{-1}$, which is comparable with that of the best Pt-spine conductors despite the fact that cobalt is a first transition series element at a much greater Co-Co spacing (3.12 Å) than that (~2.95 Å) for the conductors based on the third transition series element, Pt. Although the reflectivity shows a sharp edge at $6 \times 10^3 \text{cm}^{-1}$, it provides evidence for a small band gap. The temperature response of the conductivity of Co(pc)I is nonmetallic ($d\sigma/dT > 0$), whereas that of the isostructural Ni(pc)I is metallic. These differences can be understood by considering the effects of potentials from the I₃⁻ chains on conduction bands with different occupancies, ¹/₃ filling for Co(pc)I but ⁵/₆ filling for Ni(pc)I.

We discuss the structural, optical, charge transport, and magnetic properties of the molecular conductor (phthalocyaninato)cobalt iodide, Co(pc)I. This material, prepared by partial oxidation of Co(pc) with iodine,^{1,2} is isostructural with the low-temperature molecular metal Ni(pc)I,^{2,3} both compounds being comprised of metal-over-metal columnar stacks of partially (¹/₃) oxidized M(pc) units that are surrounded by chains of I₃⁻ ions. However, the change of incorporated metal introduces qualitative modifications in the electronic structure of the M-(L)-based molecular conductors *without* associated changes in the crystal structure. The Ni(L) compounds incorporate a d⁸ Ni²⁺ ion. Oxidation of Ni(pc) occurs at the ring, and the charge carriers of Ni(pc)I are associated with the highest-occupied delocalized π molecular orbital of pc.^{3b} For Ni(tbp)I⁴ the charge carriers are predominantly associated with the ring, but the compound exhibits a "doubly mixed valence" state, in which the hole-carriers also can hop from ring to metal. In contrast, Co(pc) incorporates a d⁷ Co²⁺ ion, and we now report that physical measurements, in particular the sign of the thermoelectric power, indicate that iodination proceeds by ¹/₃ oxidation of the metal from "Co²⁺" to

"Co^{2.33+}". Thus charge transport in Co(pc)I proceeds along a one-dimensional chain of metal centers, as in the Krogmann salts.⁵

Co(pc)I represents the first metal-spine conductor prepared from a metallomacrocycle, and to our knowledge it is the only one in which the metal ion in the parent complex is not Pt²⁺, a

(1) Taube, R. *Pure Appl. Chem.* 1974, 38, 427-438.

(2) Petersen, J. L.; Schramm, C. S.; Stojakovic, D. R.; Hoffman, B. M.; Marks, T. J. *J. Am. Chem. Soc.* 1977, 99, 286-288.

(3) (a) Schramm, C. J.; Stojakovic, D. R.; Hoffman, B. M.; Marks, T. J. *Science (Washington, D.C.)* 1978, 200, 47-48. (b) Schramm, C. J.; Scaringe, R. P.; Stojakovic, D. R.; Hoffman, B. M.; Ibers, J. A.; Marks, T. J. *J. Am. Chem. Soc.* 1980, 102, 6702-6713. (c) Martinsen, J.; Greene, R. L.; Palmer, S. M.; Hoffman, B. M. *J. Am. Chem. Soc.* 1983, 105, 677-678. (d) Martinsen, J.; Tanaka, J.; Greene, R. L.; Hoffman, B. M. *Phys. Rev. B: Condens. Matter*, 1984, 30, 6269-6276. (e) Palmer, S. M.; Ogawa, M. Y.; Martinsen, J.; Stanton, J. L.; Hoffman, B. M.; Ibers, J. A.; Greene, R. L. *Mol. Cryst. Liq. Cryst.* 1985, 120, 427-432. (f) Palmer, S. M.; Stanton, J. L.; Martinsen, J.; Ogawa, M. Y.; Heuer, W. B.; Van Wallendael, S. E.; Hoffman, B. M.; Ibers, J. A. *Mol. Cryst. Liq. Cryst.* 1985, 125, 1-11.

(4) (a) Martinsen, J.; Pace, L. J.; Phillips, T. E.; Hoffman, B. M.; Ibers, J. A. *J. Am. Chem. Soc.* 1982, 104, 83-91. (b) Ni(tbp)I = (tetrabenzoporphyrinato)nickel(II) iodide.

(5) (a) Williams, J. M.; Schultz, A. J.; Underhill, A. E.; Carnerio, K. In "Extended Linear Chain Compounds"; Miller, J. S., Ed.; Plenum Press: New York, 1982; Vol. 1, pp 73-118. (b) Miller, J. S.; Epstein, A. J. *Prog. Inorg. Chem.* 1976, 20, 1-151.

[†] Northwestern University.

[‡] IBM Research Laboratory.

[§] Nagoya University.

d^8 metal ion.^{5,6} The room-temperature conductivity of Co(pc)I is comparable with that of the best Pt-spine conductors, despite the fact the Co-Co distance is 3.12 Å, considerably longer than the Pt-Pt distance (≤ 2.95 Å) in the Pt-spine conductors. The temperature variation of the conductivity is nonmetallic but is unique among the molecular conductors. The difference between the behavior of Co(pc)I and of the metallic molecular conductor, Ni(pc)I, can be understood by considering the effects of potentials from the I_3^- chains on conduction bands of different occupancy. The Co(d_{z^2}) band of Co(pc)I is $1/3$ filled, whereas the π -orbital band of Ni(pc)I is $5/6$ filled.

Experimental Section

Preparation of Co(pc)I. Co(pc) was purchased from Eastman Kodak Co. and was triply sublimed prior to use. Iodine was obtained from Mallinckrodt and was used without further purification. Single crystals of Co(pc)I were grown in an H-tube by diffusing together 1-chloronaphthalene solutions of Co(pc) and I_2 . The resultant needles exhibit a golden luster, as opposed to Ni(pc)I and Cu(pc)I which exhibit a green luster.^{3b,7} Elemental analyses (Micro-tech Laboratories, Inc., Skokie, IL) on a number of samples from different batches are consistent with a Co(pc):I ratio of $1:1.00 \pm 0.06$ (calculated by difference). Anal. Calcd for $C_{32}H_{16}CoI_{10}N_8$: C, 55.02; N, 16.04. Found: C, 55.10; N, 16.02.

Resonance Raman Measurements. Resonance Raman spectra at ambient temperature were obtained with a spectrometer described elsewhere^{3b} on microcrystalline samples contained in spinning (1200 rpm) 5-mm Pyrex tubes. Spectra were recorded with both 5145 Å Ar⁺ and 5625 Å Kr⁺ excitation lines. The spectra were corrected, where necessary, for plasma lines.

Single-Crystal Polarized Reflectivity Spectra. Room-temperature single-crystal reflectivity spectra were recorded for Co(pc)I, both along the highly conducting needle axis and perpendicular to it, with the use of a microspectrophotometer described earlier.^{3d} Absolute reflectivities are calibrated with a SiC crystal standard. The reflectance spectra were recorded between 2.5 and 25×10^3 cm⁻¹; the crystal dimensions (0.8 mm \times 0.06 mm \times 0.06 mm) as well as surface roughness preclude measurements at lower energy.

Thermoelectric Power Measurements. Thermoelectric power (TEP) measurements along the highly conducting axis over the range 20–300 K have been obtained on an apparatus described previously.⁸ Change of temperature was accomplished by placing the copper thermal block in an Air Products LTD-3 Helitran. A low-frequency sinusoidal thermal cycling technique was used with a maximum temperature gradient across the sample of 1 K.

Charge-Transport Measurements. Crystals of length ca. 1 mm and width ca. 0.02 mm were mounted on silvered graphite fibers. Measurements at temperatures between 380 and 20 K employed an ac apparatus described earlier,⁹ a frequency of 27 Hz, and a sampling current at the crystal of 10 μ A. Variation of temperature was achieved by placing the sample in a cold-gas stream (N_2 or He).

Magnetic Susceptibility Measurements. Static magnetic susceptibilities were measured from 1.7 to 300 K on a SHE VTS-10 SQUID susceptometer. Buckets made of high-purity spectroil quartz (Thermal American Inc.) were employed. Background measurements were made over the full temperature range just prior to measurements on the sample and then checked at a few temperatures afterwards. Instrument calibration was routinely checked with $HgCo(SCN)_4$ as a standard and found to match the reported value¹⁰ to within 0.2%. The temperature-dependent studies were carried out at 10 kG on samples of ~ 30 mg. The field dependence was checked for fields up to 50 kG at 50 and 5 K and was found to be invariant in that range for a 40-mg sample.

Electron Paramagnetic Resonance Measurements. EPR spectra at ca. 9 GHz were obtained on a modified Varian E-4 spectrometer. Spectra were recorded at ambient temperature, 77 K, and 4.2 K.

X-ray Study of Co(pc)I. On the basis of Weissenberg and precession X-ray photographs Co(pc)I was assigned to the Laue group $4/mmm$. Except for a contraction of the c axis, the photographs were superimposable on those of Ni(pc)I.^{3b} Systematic absences were observed for

(6) We do not include the $Ir(CO)_2X$ compounds because their conductivity is low, even though they may be partially oxidized and do conduct to some extent. See, for example: Reis, A. H., Jr. In "Extended Linear Chain Compounds"; Miller, J. S., Ed.; Plenum Press: New York, 1982; Vol. 1, pp 157–196.

(7) Martinsen, J.; Ogawa, M. Y.; Stanton, J. L.; Hoffman, B. M.; Ibers, J. A., manuscript in preparation.

(8) Chaiken, P. M.; Kwak, J. F. *Rev. Sci. Instrum.* **1975**, *46*, 218–220.

(9) Phillips, T. E.; Anderson, J. R.; Schramm, C. J.; Hoffman, B. M. *Rev. Sci. Instrum.* **1979**, *50*, 263–265.

(10) Figgis, B. N.; Nyholm, R. S. *J. Chem. Soc.* **1958**, 4190–4191.

Table I. Crystal and Experimental Data for Co(pc)I

compound	Co(pc)I
formula	$C_{32}H_{16}CoI_{10}N_8$
fw, amu	698.37
a , Å	13.9266 (12)
c , Å	6.2466 (11)
V , Å ³	1212
Z	2
d (calcd), g/cm ³	1.91 (116 K) ^a
space group	D_{4h}^2-P4/mcc
crystal shape	needle of octagonal cross section bounded by faces of the forms {100}, {110}, {001} with separations of 0.083, 0.093, and 0.667 mm, respectively
crystal vol, mm ³	0.00345
radiation	Cu K α filtered at the receiving aperture with Ni (λ (Cu K α_1) = 1.54056 Å)
μ , cm ⁻¹	162.8
transmission factors	0.162–0.417
takeoff angle, deg.	4.5
receiving aperture	4.0 mm wide \times 4.5 mm high; 34 cm from crystal
scan speed, deg 2 θ /min	2
background counts	20s, with rescan option ^b
data collected	$h \geq k \geq 0; \pm l$
unique data	540
unique data with $F_o^2 > 3\sigma(F_o^2)$	451
no. of variables	66
R on F_o^2	0.055
R_w on F_o^2	0.082
R on $F_o, F_o^2 > 3\sigma(F_o^2)$	0.036
R_w on $F_o, F_o^2 > 3\sigma(F_o^2)$	0.044
error in observation of unit wt, e ²	1.8

^aThe low-temperature system is based on a design by J. C. Huffman (Ph.D. Thesis, Indiana University, 1974). ^bThe diffractometer was run under the disk-oriented Vanderbilt system (Lenhart, P. G. *J. Appl. Crystallogr.* **1975**, *8*, 568–570).

Table II. Positional Parameters for Co(pc)I

atom	x	y	z
I	1/2	1/2	1/4
Co	0	0	0
N(1)	0.12490 (30)	0.05802 (28)	0
N(2)	0.08275 (29)	0.22716 (30)	0
C(1)	0.14393 (37)	0.15440 (36)	0
C(2)	0.24723 (35)	0.17010 (34)	0
C(3)	0.30341 (37)	0.25389 (37)	0
C(4)	0.40229 (37)	0.24244 (39)	0
C(5)	0.44426 (34)	0.15122 (38)	0
C(6)	0.38881 (36)	0.06811 (38)	0
C(7)	0.28937 (36)	0.07929 (36)	0
C(8)	0.21060 (32)	0.01079 (40)	0

reflections $0kl$ and hhl with l odd, consistent with space groups $P4/mcc$ or $P4cc$. The successful refinement of the structure supports the choice of space group D_{4h}^2-P4/mcc . The cell constants of $a = 13.927$ (1) Å and $c = 6.247$ (1) Å at 116 K were found by a least-squares refinement¹¹ of 17 reflections that had been centered on a FACS-I diffractometer with the use of Cu K α radiation. Co(pc)I crystallizes in the same space group as Ni(pc)I³ and Ni(tpb)I⁴ and displays similar X-ray photographs. That Co(pc)I and Ni(pc)I are isostructural was confirmed upon solution of the structure of Co(pc)I. In addition to normal Bragg scattering, diffuse scattering was observed on oscillation and precession photographs of Co(pc)I in planes perpendicular to the c^* axis. Diffuse scattering in similar systems, most notably that of Ni(pc)I, has been interpreted in terms of disorder along the iodine chain.

Intensity data for the Bragg scattering were collected at 116 (3) K by the θ - 2θ scan technique and were processed with a value of 0.03 for p ¹¹ by methods standard in this laboratory.¹² No significant change was detected in the intensities of six standard reflections that were measured

(11) Corfield, P. W. R.; Doedens, R. J.; Ibers, J. A. *Inorg. Chem.* **1967**, *6*, 197–204.

(12) See, for example: Waters, J. M.; Ibers, J. A. *Inorg. Chem.* **1977**, *16*, 3273–3277.

Table V. Observed Bond Distances (Å) and Angles (deg) for Co(pc)I

Distances, Å			
Co-N(1)	1.918 (4)	C(2)-C(7)	1.394 (7)
N(1)-C(1)	1.368 (6)	C(3)-C(4)	1.386 (7)
N(1)-C(8)	1.363 (6)	C(4)-C(5)	1.398 (8)
N(2)-C(1)	1.324 (7)	C(5)-C(6)	1.392 (7)
N(2)-C(8)	1.323 (7)	C(6)-C(7)	1.394 (7)
C(1)-C(2)	1.455 (7)	C(7)-C(8)	1.454 (7)
C(2)-C(3)	1.405 (7)		
Angles, deg			
N(1)-Co-N(1)'	90.00	C(2)-C(3)-C(4)	117.2 (5)
Co-N(1)-C(1)	126.1 (3)	C(3)-C(4)-C(5)	121.3 (5)
Co-N(1)-C(8)	126.2 (3)	C(4)-C(5)-C(6)	121.6 (5)
C(1)-N(1)-C(8)	107.7 (4)	C(5)-C(6)-C(7)	117.3 (5)
C(1)-N(2)-C(8)	120.0 (4)	C(2)-C(7)-C(6)	121.3 (5)
N(1)-C(1)-N(2)	128.8 (5)	C(2)-C(7)-C(8)	106.1 (4)
N(1)-C(1)-C(2)	109.8 (4)	C(6)-C(7)-C(8)	132.6 (5)
N(2)-C(1)-C(2)	121.4 (4)	N(1)-C(8)-N(2)	128.9 (4)
C(1)-C(2)-C(3)	132.5 (4)	N(1)-C(8)-C(7)	110.1 (5)
C(1)-C(2)-C(7)	106.2 (4)	N(2)-C(8)-C(7)	121.0 (4)
C(3)-C(2)-C(7)	121.3 (4)		

every 100 reflections. A total of 540 unique reflections was measured; of these 451 have $F_o^2 > 3\sigma(F_o^2)$. Experimental details and crystal data are given in Table I.

Starting positional parameters of the non-hydrogen atoms were those of Ni(pc)I. The full matrix anisotropic refinement on F converged to values of R and R_w of 0.046 and 0.062, respectively. Next, hydrogen positions were idealized ($C-H = 0.95$ Å) and were not varied through the remainder of the refinement. Each hydrogen atom was given a thermal parameter of 1 Å² greater than that of the carbon atom to which it is bonded. The final refinement on F_o^2 with variable anisotropic thermal parameters for all non-hydrogen atoms and a variable extinction parameter led to values for R and R_w on F_o^2 of 0.055 and 0.082, respectively. In this cycle of refinement there were 66 variables and 540 observations (including $F_o^2 < 0$). The highest peak (0.6 e/Å³) in the final difference electron density map is located near the Co atom. Smaller peaks lie between the I atoms.

The final positional parameters are given in Table II. Thermal parameters are given in Table III,¹³ and a list of $10|F_o|$ vs. $10|F_c|$ is given in Table IV.¹³ In this listing an entry with F_o negative symbolizes a reflection having $F_o^2 < 0$.

Results

Description of the Structure. The Co(pc)I structure is essentially identical with that of Ni(pc)I. The M-N(1) distance in Co(pc)I is 1.918 (4) Å compared with 1.887 (6) Å in Ni(pc)I. This is the largest difference between the bond distances and angles of the two metallomacrocycles. Observed bond distances and angles are listed in Table V. As in Ni(pc)I, the crystal packing of Co(pc)I consists of linear chains of iodine atoms segregated from macrocycle stacks, both of which run parallel to the c axis. The iodine chains run in channels formed by the benzo groups of the neighboring Co(pc) units. The two Co(pc) molecules in the unit cell are staggered by 40°. Each Co(pc) unit is on a site of $4/m$ symmetry and consequently is constrained to be planar with the normal to the plane parallel with the stacking axis. Figure 1 shows a view of the Co(pc) stack. The metal-over-metal stacking that results is a characteristic of such iodine-oxidized metallomacrocyclic systems, but the intrastack spacing (3.123 (1) Å) is unusually small. The iodine atom is on a site of 422 symmetry. The thermal parameter of the iodine atom is nearly twice as large along the chain direction as it is perpendicular to the chain. A similar result in Ni(pc)I has been attributed to ordered chains of I_3^- that are disordered with respect to their neighbors. Detailed analysis of the diffuse X-ray scattering that results from this disorder was made for Ni(pc)I^{3b} and is not repeated here.

In the context of the measurements discussed below, the very short intrastack spacing and the electronic properties of Co(pc)I indicate relatively strong electronic interactions between Co atoms. The root-mean-square amplitude of vibration of the Co atom along the chain ($U_{||} = 0.141$ (3) Å), although not unusual in magnitude,

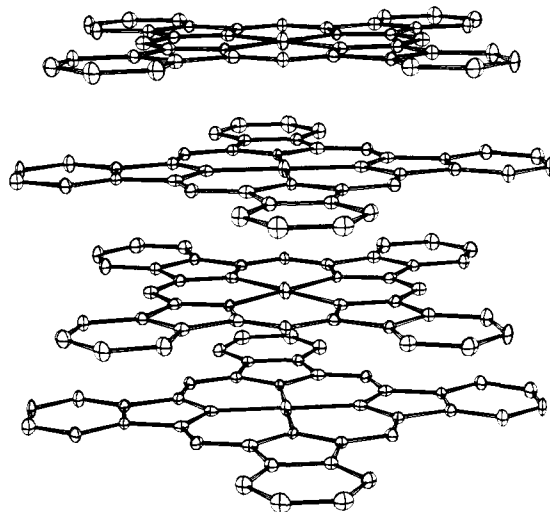


Figure 1. Perspective view into a Co(pc) stack. Hydrogen atoms have been omitted.

is larger than in the direction perpendicular to the stack ($U_{\perp} = 0.094$ (3) Å). However, because $U_{||}/U_{\perp}$ is roughly the same here as for the Ni atom in Ni(pc)I where Ni-Ni interaction is not expected, no such Co-Co interaction is required to explain the value of $U_{||}/U_{\perp}$. The final difference electron density map of Co(pc)I shows regions of electron density between atoms of the pc ring and good agreement between chemically equivalent portions of the ring. However, a region of positive electron density between the two adjacent Co atoms in the unit cell is not observed.

Resonance Raman Spectroscopy. The resonance Raman spectrum of Co(pc)I exhibits a sharp fundamental peak at 109 cm⁻¹, with an overtone progression of peaks at 214, 322, and 438 cm⁻¹. This pattern is characteristic of a system containing linear chains of symmetrical triiodide ions.¹⁴ The absence of any observable features at 212 cm⁻¹ (above the expected intensity of the overtone band) and 167 cm⁻¹ rule out I_2 and I_5^- , respectively, as the predominant iodine form. Thus the proper formulation of Co(pc)I, as indeed of all of the M(pc)I systems studied to date, is $[Co(pc)]_2[Co(pc)]^+I_3^-$, or in the mixed valence form $[Co(pc)]^{0.33+}[I_3^-]_{0.33}$.

There are some subtle but interesting differences between the Raman measurements of Co(pc)I and those of the other M(pc)I systems ($M = H_2^+, Fe, Ni, Cu, Pd, Pt$).^{2,7,15} The signal obtained with the 5145 Å Ar⁺ excitation line is much weaker for $M = Co$ than for the other systems. As disclosed by the reflectivity measurements presented below, this weakening arises from a loss of resonance enhancement because of a bathochromic shift of the triiodide $\sigma_u^* \leftarrow \sigma_g$ optical transition in the Co(pc)I system relative to the other M(pc)I systems. Indeed, the spectrum obtained with the 5682 Å Kr⁺ line is more intense than that with the 5245 Å Ar⁺ line, although the Kr⁺ line is much weaker than the Ar⁺ line.

In spite of the relatively large effect of the contracted c spacing on the optical properties of triiodide chains in Co(pc)I, there is virtually no effect on the vibrational frequency of the totally symmetric stretching mode of the triiodide system. Co(pc)I, with a lattice c spacing of 6.247 (1) Å, exhibits a fundamental with a frequency within experimental error of that for Ni(pc)I, which has a lattice c spacing of 6.41 (1) Å.¹⁶ This invariance is consistent with results obtained from a number of model compounds.¹⁷ They show the iodine stretching frequencies to be insensitive to the I-I distances.

(14) Marks, T. J. *Ann. NY Acad. Sci.* **1978**, 594-616.

(15) Schramm, C. J. Ph.D. Thesis, Northwestern University, Evanston, IL, 1979.

(16) The unit cell constants of $a = 13.86$ (1) Å and $c = 6.41$ (1) Å were recently determined for Ni(pc)I at 105 K by least-squares refinement of 25 reflections on an Enraf-Nonius CAD-4 X-ray diffractometer.

(17) (a) Mizuno, M.; Tanaka, J.; Harada, I. *J. Phys. Chem.* **1981**, *85*, 1789-1794. (b) Torrance, J. B.; Scott, B. A.; Welber, B.; Kaufman, F. B.; Seiden, P. E. *Phys. Rev. B: Condens Matter* **1979**, *19*, 730.

(13) Supplementary material.

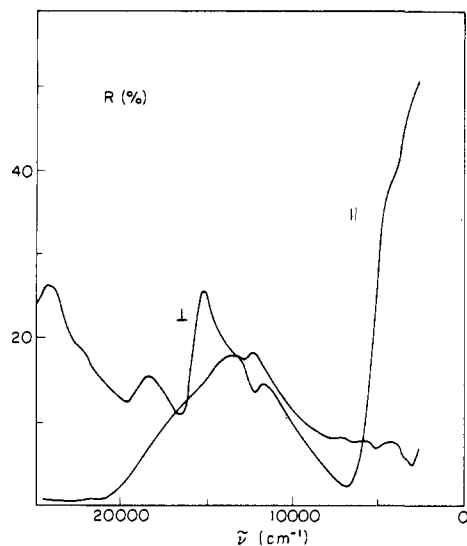


Figure 2. Single-crystal polarized reflectance spectra for Co(pc)I.

Single-Crystal Polarized Reflectivity Measurements. The single-crystal polarized reflectance spectra are shown in Figure 2. Although the spectrum obtained with the electric field vector perpendicular to the highly conducting (*c*) axis is not as well resolved in Co(pc)I as in a similar spectrum obtained for Ni(pc)I,^{3d} by analogy it is reasonable to assign the main features at 24, 18.5, and $15.5 \times 10^3 \text{ cm}^{-1}$ to the in-plane $\pi g^* \leftarrow \pi u$ transitions of the pc π system.¹⁸ At low frequency the reflectivity is relatively small and does not exhibit features readily attributable to intraband transitions; the feature at $3.5 \times 10^3 \text{ cm}^{-1}$ probably is an artifact that arises from the poor surface quality of the crystal. The spectrum recorded with the electric field polarized parallel to the highly conducting axis shows a strong peak, centered at $13.5 \times 10^3 \text{ cm}^{-1}$, that we assign to a $\sigma u^* \leftarrow \sigma g$ transition of the triiodide chain.¹⁷ This transition in Co(pc)I shows an appreciable bathochromic shift relative to that in Ni(pc)I ($18.5 \times 10^3 \text{ cm}^{-1}$) that occurs because the *average* I-I spacing in Co(pc)I is less than that in Ni(pc)I.

The near infrared region is characterized by a sharp increase in reflectivity at $6 \times 10^3 \text{ cm}^{-1}$. The occurrence of this feature in parallel polarization and its absence in perpendicular polarization is consistent with this material being a quasi-one-dimensional conductor with transport along the stacking *c* axis. If the reflectivity were to continue to rise steeply to lower energy, as in Ni(pc)I, it would indicate that Co(pc)I is a metallic conductor; however, the reflectivity in the $3\text{--}5 \times 10^3 \text{ cm}^{-1}$ region shows a broad shoulder, a typical pattern of a higher energy tail of a transition with an energy gap. In Pt-spine complexes, such as KCP, the band-to-band transition of the mixed valence chain is found at $1.5 \times 10^3 \text{ cm}^{-1}$, even though a sharp Drude-type edge is found at $17 \times 10^3 \text{ cm}^{-1}$.⁵ The optical reflectivity of Co(pc)I thus provides evidence of a small band gap in the lower energy region.

Thermoelectric Power. The Seebeck coefficient (*S*) measured along the conducting axis of Co(pc)I is negative, and becomes increasingly so as the temperature is lowered to ca. 150 K (Figure 3). The sign of the predominant charge carriers is given by the sign of the thermoelectric power, and the thermoelectric power thus identifies electrons as the predominant charge carriers in Co(pc)I. This result contrasts with the positive value of *S* for Ni(pc)I and Cu(pc)I.^{3d,7} There the macrocycle ring is the site of oxidation and the charge carriers are associated with the highest-occupied π molecular orbital of the ring. The valence band formed from this orbital would be doubly occupied in a neutral M(pc) stack (Figure 4). Oxidation by $1/3$ e per site, as in Ni(pc)I, leads to a $5/6$ filled band, which corresponds to a band in which charge transport is associated with a band $1/6$ filled with positive

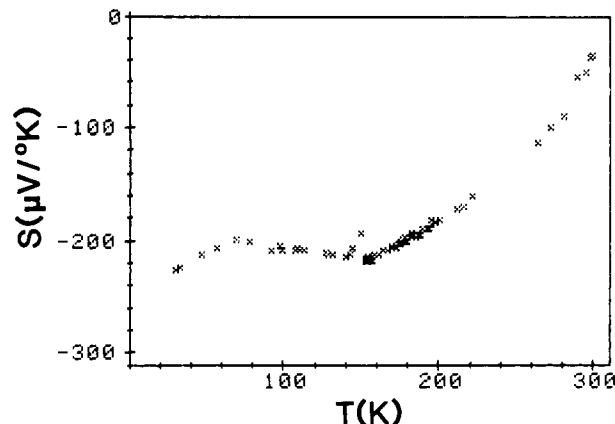


Figure 3. Thermoelectric power of Co(pc)I. The Seebeck coefficient, *S* ($\mu\text{V/K}$), is plotted as a function of *T*.

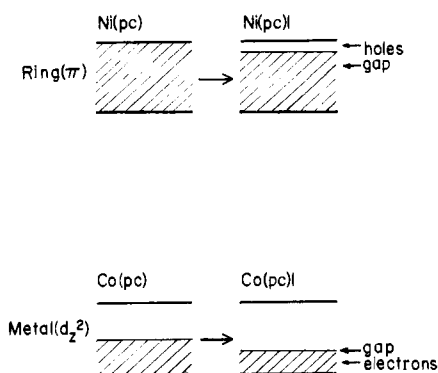


Figure 4. Schematic diagram showing partial oxidation of the highest-occupied molecular orbitals of Ni(pc)I and Co(pc)I. For Ni(pc)I a filled band of π electrons of the (pc) ring loses $1/3$ e per site on partial oxidation, giving a band $5/6$ full, with holes as the carriers. For Co(pc)I, the band that is oxidized is the half-filled Co- d_{z^2} band. Upon loss of $1/3$ e per site, the band becomes $1/3$ filled with electrons as the carriers. In each case the energy level nearest to the Fermi level at which a trimerized iodine chain would create an energy gap is indicated.

“holes” and a positive Seebeck coefficient. The negative sign of *S* for Co(pc)I is interpretable only in terms of oxidation at, and charge transport along the Co spine. The valence band formed from the singly occupied cobalt d_{z^2} orbital in a neutral Co(pc) stack would be $1/2$ filled (Figure 4). Oxidation by $\rho = 1/3$ e per site would give a cobalt d_{z^2} band that is $1/3$ filled; conduction would be associated with electrons and *S* would be negative. Thus the negative Seebeck coefficient of Co(pc)I identifies cobalt as the site of oxidation, and a descriptive formulation of the compound is $[\text{Co}^{2.33+}(\text{pc})](\text{I}_3^-)_{0.33}$. This conclusion is in accord with electrochemical studies of M(pc) in solution,¹⁹ although our study through use of solid-state electrochemical cells of the formation energies of M(pc)I did not indicate any significant energetic differences between ring-oxidized Ni(pc)I (or Cu(pc)I) and metal-oxidized Co(pc)I.²⁰

The temperature dependence of *S* (Fig. 4) does not follow the prediction of any simple model. The linear ($S \propto T$) approach toward zero expected in systems with metallic conductivity, and found in Ni(pc)I,^{3d} is not observed. Instead, the behavior is more like that expected for a semiconductor²¹ ($S \propto E_g/T$) with a gap E_g ; however, the constant value of $-20 \mu\text{V/K}$ between ca. 50 and 150 K then is unusual. The nature of the static susceptibility, discussed below, suggests the Coulomb interaction (*U*) between carriers on a single site may be comparable with or greater than

(19) Wolberg, A.; Manassen, J. *J. Am. Chem. Soc.* **1970**, *92*, 2982–2991.

(20) Euler, W. B.; Melton, M. E.; Hoffman, B. M. *J. Am. Chem. Soc.* **1982**, *104*, 5966–5971.

(21) Kittel, C. “Introduction to Solid State Physics”; John Wiley & Sons, Inc.; New York, 1976; pp 237–238.

(18) Lever, A. B. P. *Adv. Inorg. Chem. Radiochem.* **1965**, *7*, 28–114.

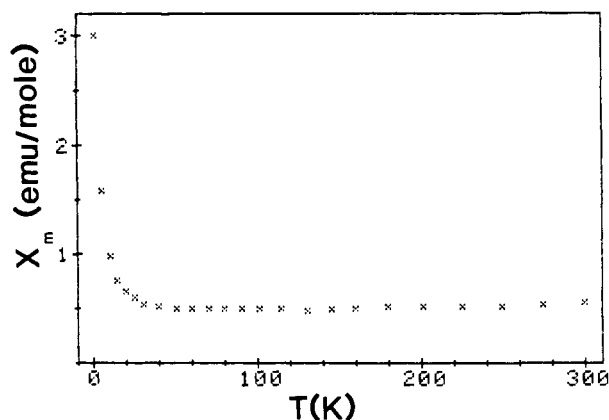


Figure 5. Magnetic susceptibility, χ (emu/mol) $\times 10^{-3}$, vs. temperature for Co(pc)I.

the transfer integral (t) in Co(pc)I. In this case at temperatures where $kT \gg t$ one expects a constant thermopower given by²²

$$S = -\frac{h}{|e|} \ln [2(1 - \delta)/\delta]$$

where δ is the site oxidation and the negative sign applies when the band is less than $1/2$ filled and the carriers are electrons. For Co(pc)I, $\delta = 1/3$ and this model gives a constant value, $S \approx -120 \mu\text{V/K}$, near room temperature. Although at high-temperature S is not constant and in fact becomes smaller than $-120 \mu\text{V/K}$ (Figure 4), the temperature response of S for Co(pc)I is similar to that found in the organic conductors where a gap created by Coulomb interactions is thought to be important.²² Although we do not understand the details, we conclude that $S(T)$ is qualitatively explained by a gap in the electronic band structure, with the possibility that defect states in the gap are the cause of the low-temperature behavior. We argue below that the gap is an effect of the iodine chains on the $1/3$ filled Co(d_{2z}) band.

Magnetic Susceptibility. The static magnetic susceptibility of Co(pc)I, measured at 293 K and corrected for the diamagnetism of the ring and the metal, is 5.00×10^{-4} emu/mol, which is equivalent to 0.40 spins/macrocycle when $S = 1/2$ and $g = 2$. This value, though ~ 2.5 times larger than that for Ni(pc)I, does not reflect the full magnetization expected of at least 1 spin/site from Co^{2+} . This reduced susceptibility demonstrates a strong interaction between cobalt atoms and is consistent with assignment of the site of oxidation as the metal (Co^{3+} is diamagnetic) rather than the ring.

The temperature dependence of the susceptibility has been measured between 1.7 and 300 K (Figure 5). In the range 30 to 300 K the susceptibility is nearly temperature independent, exhibiting only a 5% decrease with decreasing temperature. Below 30 K a Curie "tail" is observed; however, as in Ni(pc)I, this is associated with surface defects, since the magnitude of this tail is dependent on the extent of pumping on the sample prior to entry into the SQUID sample chamber. Such a weakly temperature-dependent paramagnetism typically is interpreted in terms of a Pauli susceptibility of a degenerate electron gas. The expression in the one-dimensional tight-binding theory for a half-filled band that relates the transfer integral t and the Pauli susceptibility χ_p is²³

$$t = N\beta^2 / [\chi_p \pi \sin(\rho\pi/2)]$$

where β is the Bohr magneton, N is Avogadro's number, and ρ is the degree of oxidation. The value of 5.00×10^{-4} emu/mol for χ_p and $1/3$ for ρ yields $t = 0.024$ eV and a bandwidth of 0.10 eV. However, this value is so small that the susceptibility associated with such a bandwidth would not be temperature invariant.

(22) Mortenson, K.; Conwell, E. M.; Fabre, J. M. *Phys. Rev. B: Solid State* **1983**, *28*, 5856-5862.

(23) (a) Shiba, H. *Phys. Rev. B: Solid State* **1972**, *6*, 930-938. (b) Torrance, J. B.; Tomkiewicz, Y.; Silverman, B. D. *Phys. Rev. B: Solid State* **1977**, *15*, 4738-4749.

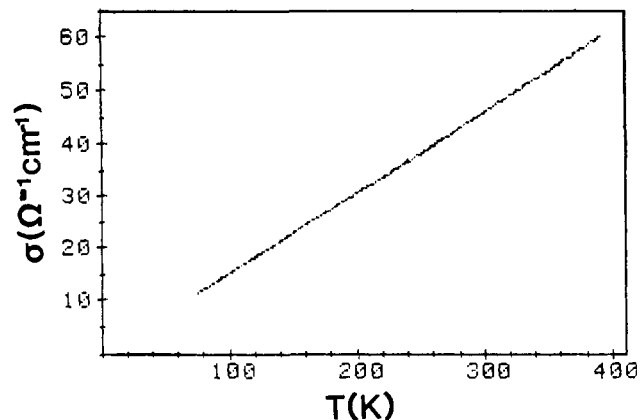


Figure 6. Temperature dependence of the conductivity of a single crystal of Co(pc)I.

There are two obvious explanations for this discrepancy. Possibly the susceptibility is enhanced because low-lying excited states on the cobalt center contribute a temperature-independent (van Vleck) paramagnetism. A more likely alternative is that the reduced conductivity and high susceptibility of Co(pc)I reflect strong Coulomb correlations among the electron carriers associated with the " $\text{Co}^{2.33+}$ " ions. Strong Coulomb correlations and an enhanced susceptibility do not occur in Ni(pc)I, where the carriers are delocalized on the ring, but they would be expected in Co(pc)I, a quasi-one-dimensional conductor that has the carriers confirmed to a conducting metal spine.

We find that the susceptibility can be described in terms of a Heisenberg chain of exchange-coupled spins having $2/3$ of a spin per site^{23b} and an exchange integral $J = 0.011$ eV. Such spin coupling in a molecular conductor can be interpreted within the Hubbard model for a one-dimensional chain and would arise when the on-site Coulomb interaction, U , is large compared with the intersite electron transfer matrix element, t , leading to an exchange coupling $J = 2t^2/U$. For heuristic purposes we obtain the estimate, $t \sim 0.07$ eV, by assuming $U \sim 1$ eV, which might be expected to be appropriate for carriers on a metal spine.

This treatment thus leads to a reasonable picture of the different magnetic properties of Ni(pc)I and Co(pc)I. In both materials there is an appreciable matrix element, t , for charge transfer. However, the carrier repulsion term, U , is low when the carriers are associated with a delocalized π orbital on the ring, but it is large when the carriers are associated with a localized d_{2z} orbital on a cobalt center.

Electron Paramagnetic Resonance Measurements. The EPR spectrum of Co(pc)I at 298 K exhibits a single weak signal at $g = 2.0027$, with a line width $\Gamma = 4.5$ G. Integration of this signal results in only $\sim 2 \times 10^{-4}$ spins per macrocycle, and as such it is readily assignable to an impurity. Spectra recorded at 77 and 4.2 K fail to show any new features, and thus we conclude that the intrinsic charge carriers are EPR silent, perhaps because of short relaxation times that make the signal very broad. In the other M(pc)I systems where the oxidation has occurred on the ring, the carriers have been EPR visible, even when the potential exists for strong coupling with a paramagnetic center, such as for Cu(pc)I.^{3e,7} Thus the lack of a signal in Co(pc)I is unusual and is entirely consistent with oxidation of Co rather than oxidation of the pc ring.

Charge-Transport Measurements. The four-probe conductivity of single crystals of Co(pc)I at 298 K, measured along the stacking axis on 17 samples, cluster tightly in the range 45 to 50 $\Omega^{-1} \text{cm}^{-1}$. This is an order of magnitude smaller than conductivities for most other M(pc)I systems, even though the intrastack spacing in Co(pc)I is slightly less than that in Ni(pc)I,^{3f} but it is similar to those for the platinum metal-spine conductors.^{5,24} Figure 6 shows the temperature response of the conductivity for a typical Co(pc)I crystal over the range 20-380 K to be nonmetallic ($d\sigma/dT > 0$),

(24) Kuse, D.; Zeller, H. R. *Phys. Rev. Lett.* **1971**, *27*, 1060-1063.

unlike Ni(pc)I. Generally a nonmetallic molecular conductor exhibits an exponential temperature dependence of $\sigma(T)$ because the carrier density or mobility or both are activated. However, Co(pc)I shows an unprecedented, approximately linear variation of $\sigma(T)$ with temperature.

Discussion

Co(pc)I is a molecular conductor analogous to the platinum chain conductors rather than to other M(pc)I systems. Indeed Co(pc)I appears to be the first authenticated metal-spine molecular conductor that is not based on a platinum complex, and the conductivity is high even though the Co-Co spacing is 3.12 Å as opposed to the shorter spacings in the platinum-based conductors (≤ 2.95 Å). Nevertheless, the room-temperature conductivity of Co(pc)I is much less than that of the π -orbital conductor, Ni(pc)I. Moreover, although the exact form of $\sigma(T)$ for Co(pc)I is not understood, the nonmetallic behavior, with $\sigma(T) \rightarrow 0$ as $T \rightarrow 0$, is qualitatively in agreement with the inference drawn from the thermopower and reflectivity measurements that this material is unlike Ni(pc)I in that it shows a gap in the electronic band structure at the Fermi energy.

Although several factors associated with one-dimensional conductors can contribute to the formation of a gap,²⁵ we consider that the potentials set up by the iodine substructure are the most prominent, and that the difference between Co(pc)I and Ni(pc)I can be understood by considering the influence of the iodine substructure on electronic bands that have different occupancies in the two conductors.

A channel formed by M(pc) stacks in the M(pc)I structure contains a chain of iodine atoms that is trimerized to form a chain

of regular I_3^- species. The electrostatic potential from such a chain tends to create a gap in the conduction band at an energy level corresponding to $1/3$ and $2/3$ filling (Figure 4). However, as noted above, oxidation of Ni(pc) to form Ni(pc)I leads to a $5/6$ filled π molecular orbital band, whereas Co(pc)I contains a $1/3$ filled Co(d_{z^2}) band. Thus, gap formation in Ni(pc)I would have little effect on σ , whereas for Co(pc)I it would tend to cause nonmetallic behavior, as observed. Moreover, one would not expect Co(pc)I to exhibit a well-defined gap and typical semiconductive behavior. The iodine chains in the M(pc)I, though individually ordered, are disordered with respect to each other. Thus, we take the anomalous temperature response to $\sigma(T)$ for Co(pc)I to reflect a gap at the Fermi surface that is smeared out because the Co(pc) stacks are subject to a random potential from the disordered iodine chains.

In summary, the entire set of differences between Co(pc)I and Ni(pc)I can be discussed self-consistently by treating the former to be a metal-spine conductor, whereas carriers on the latter are associated with the pc ring.

Acknowledgment. The work at Northwestern University was supported by the Northwestern University Materials Research Center under the National Science Foundation NSF-MRL program (Grant DMR 82-16972) and through the Solid State Chemistry Program of the National Science Foundation (DMR8116804 to B.M.H.). The authors thank Dr. S. M. Palmer for Resonance Raman measurements.

Registry No. Co(pc)I, 30289-99-7.

Supplementary Material Available: Tables III (positions and anisotropic thermal parameters for non-hydrogen atoms; hydrogen atom positions and isotropic thermal parameters) and IV (structure amplitudes) for Co(pc)I (4 pages). Ordering information is given on any current masthead page.

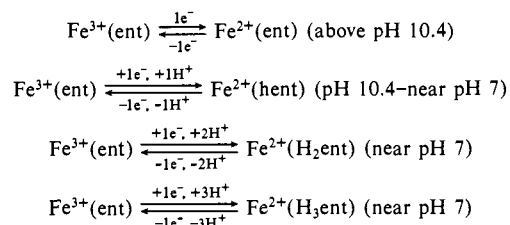
(25) (a) Jerome, D.; Schulz, H. J. In "Extended Linear Chain Compounds"; Miller, J. S., Ed.; Plenum Press, New York, 1982; Vol 2, pp 159-204. (b) Comès, R.; Lambert, M.; Launais, H.; Zeller, H. R. *Phys. Rev. B: Solid State* 1973, 8, 571-575.

The pH-Dependent Reduction of Ferric Enterobactin Probed by Electrochemical Methods and Its Implications for Microbial Iron Transport¹

Chi-Woo Lee, David J. Ecker, and Kenneth N. Raymond*

Contribution from the Department of Chemistry, University of California, Berkeley, California 94720. Received March 4, 1985

Abstract: The coordination chemistry of ferric enterobactin has been probed by cyclic voltammetry, normal and differential pulse polarography, and controlled-potential electrolysis. The formal potential of the iron(3+/2+) couple for the enterobactin complex is found to be -1.03 V vs. SSCE (-0.79 V vs. NHE) at pH 7.4 in a solution containing 0.4 M NaClO₄ and 20 mM phosphate buffer. The first protonation constant of ferric enterobactin is 10^{4.8}; therefore in the pH range studied (6-11.4) ferric enterobactin is present entirely as [Fe(ent)]³⁺. Thus the pH dependence of the formal potentials in this region is due entirely to protonation of the *ferrous* complex. Four regions involving one-electron transfers have been identified. These reactions are



The implications of these data for the mechanism of enterobactin-mediated iron transport in microorganisms which utilize this siderophore are presented.

Enterobactin is a siderophore (microbial iron transport agent) whose coordination chemistry²⁻⁶ and mechanism(s) of microbial

iron transport⁷⁻⁹ have been of recent interest, largely because of the important role iron availability plays in bacterial growth and